Int. J. Heat Mass Transfer. Vol. 19, pp. 1205–1214. Pergamon Press 1976. Printed in Great Britain

CIRCUMFERENTIALLY LOCAL AND AVERAGE TURBULENT HEAT-TRANSFER COEFFICIENTS IN A TUBE DOWNSTREAM OF A TEE

D. A. WESLEY and E. M. SPARROW
Department of Mechanical Engineering, University of Minnesota, Minneapolis, MN 55455, U.S.A.

(*Received* 22 *March* 1976)

Abstract—Experiments were performed to determine heat-transfer coefficients both around the circumference and along the length of a heated tube situated downstream of a flow-splitting tee. The flow arrangement was such that air was delivered to the center port of the tee by a long unheated hydrodynamic development section and exited the tee via its two end ports. Identical heated tubes, each with its own flow control, were respectively attached to each exit port. One of the heated tubes served as a primary test section. The experiments were performed at several fixed primary test section Reynolds numbers and, at each Reynolds number, the flow through the secondary exit was varied systematically. The circumferential average heat-transfer coefficients in the thermal entrance region were found to be much larger than those for a conventional axisymmetric tube flow. Furthermore, the length of the thermal entrance region was substantially greater owing to the presence of the tee. Circumferential variations of the heat-transfer coefficient were confined to the initial portion of the entrance region, with circumferential uniformity being attained within about eight diameters from the center of the tee. At the first measurement station (two diameters from the center of the tee), the circumferential distributions exhibited deviations of up to 30% from the circumferential average.

NOMENCLATURE

- D, I.D. of test section tube;
- h_{fd}, fully developed heat-transfer coefficient;
- $h_x(\theta)$, circumferentially local heat-transfer coefficient, equation (1);
- $\bar{h}_x$, circumferential average heat-transfer coefficient, equation (7);
- k, thermal conductivity of air;
- k_w, thermal conductivity of tube wall;
- $\dot{m}_1$, mass flow rate in primary test section;
- $\dot{m}_2$, mass flow rate in secondary test section;
- Nu_{fd}, fully developed Nusselt number, $h_{fd}D/k$;
- $\overline{Nu}_x$, circumferential average Nusselt number, $\bar{h}_x D/k$;
- Q_l, heat loss to environment;
- $q_x(\theta)$, circumferentially local heat flux;
- $\bar{q}_x$, circumferential average heat flux;
- q''', volumetric heat generation rate;
- R_i, inner radius of test section tube;
- R_o, outer radius of test section tube;
- R_m, mean radius, $\frac{1}{2}(R_o+R_i)$;
- Re_1, primary test section Reynolds number, $4\dot{m}_1/\mu\pi D$;
- S, flow split number, $\dot{m}_2/\dot{m}_1$;
- T_{bx}, local bulk temperature;
- $T_{wx}(\theta)$, local wall temperature at angle θ;
- $\bar{T}_{wx}$, circumferential average wall temperature;
- T_∞, environment temperature;
- t, tube wall thickness;
- X, axial coordinate measured from center of tee.

Greek symbols

- θ, angular coordinate;
- μ, viscosity of air.

Subscript

- e, thermal entrance length.

INTRODUCTION

TURBULENT heat transfer in tubes is, perhaps, the most commonly encountered convective heat-transfer situation. As a consequence, the heat-transfer characteristics of turbulent tube flows have been subjected to extensive investigation. In the main, these investigations have concerned themselves with hydrodynamic entrance conditions which give rise to axisymmetric velocity distributions. In practice, however, more complex flow fields are encountered. A tee is an example of a tube inlet configuration which yields a non-axisymmetric velocity distribution as well as a secondary flow superposed on the axial flow. The present experimental investigation, conducted with air as the working fluid, is concerned with the heat-transfer characteristics for turbulent flow in a tube downstream of a tee.

The objectives of the research are to obtain results that are both of practical and of fundamental interest. The former includes Nusselt number distributions and entrance lengths for a wide range of flow conditions. With respect to the latter, it may be noted that the unsymmetric velocity profiles and the secondary flow associated with the presence of the tee serve to activate circumferential turbulent transport. Careful measurements have been made of the corresponding circumferential variations of the heat-transfer coefficient.

There are several inflow/outflow arrangements by which a tee can be coupled to a piping system. In the present research, air was supplied to the center port of a tee by means of a long, unheated hydrodynamic development tube. The two end ports of the tee served

as exits, and a uniformly heated tube was attached to each exit port. One of the heated tubes, designated as the primary test section, was employed for the heat-transfer and temperature measurements. The other heated tube will be referred to as the secondary test section.

The apparatus was designed to enable the flow entering the tee to be arbitrarily subdivided between the two test sections. The experiments were conducted so that for each fixed Reynolds number in the primary test section, the flow in the secondary test section was systematically varied from zero to the maximum consistent with the instrumentation.

For the aforementioned inflow/outflow arrangement, the flow entering the tee behaves like a jet which impinges on the wall of the tee opposite the inlet. At first, the flow is concentrated near the wall on which it impinges. As the fluid streams out of the tee into the respective test section tubes, it tends to move circumferentially (i.e. to climb the wall) as well as axially, owing to cross sectional pressure variations set up by the impingement and deflection. This secondary motion plays an important role in redistributing the flow which was initially concentrated near the impingement wall. Ultimately, both the secondary flow and the nonsymmetries in the velocity profile are dissipated by the action of viscosity and turbulent diffusion.

A literature search did not reveal any prior publications dealing with the heat-transfer characteristics for turbulent flow downstream of a flow-splitting tee. A study that is somewhat related to the present work is that of Mills [1], who measured the axial variation of the heat-transfer coefficient along a uniformly heated tube fitted with various fluid inlet configurations, one of which was a tee. Air from the laboratory room was drawn through the inlet fitting into the test section. No mention is made of which ports of the tee served as inflow and outflow passages but, whatever the flow arrangement, it was different from that studied here. Also somewhat related to the present investigation, especially to the case where there is no flow in the secondary test section, are studies of heat-transfer downstream of 90-degree mitered elbows and bends [2–4].

The velocity field downstream of a flow-splitting tee was investigated by means of a laser-Doppler velocimeter [5]. The experiments were restricted to laminar flow and to a single ratio of the flows through the exit ports.

EXPERIMENTAL APPARATUS AND INSTRUMENTATION

The design and fabrication of the experimental apparatus was performed with painstaking care and attention to detail. The essential features of the apparatus and instrumentation will be described here whereas other details, omitted due to space limitations, are available in [6].

Apparatus

An overall description of the apparatus is facilitated by following the path of the airflow. Air from a central compressor was dried and then delivered to the laboratory, where it passed through an optional preheater, a pressure regulator, control valves, and a filter. Then, as indicated schematically in the left-hand diagram of Fig. 1, the air entered a long hydrodynamic development section, the downstream end of which mated with the central port of a tee. As noted earlier, both of the end ports of the tee served as exits, and identical electrically heated tubes were attached to each exit. The airflow entering the tee was subdivided between the two exits and passed through the respective tubes. At the downstream end of each tube was a mixing box, a control valve, and a rotameter. Adjustment of these control valves enabled the flow to be arbitrarily apportioned between the tubes.

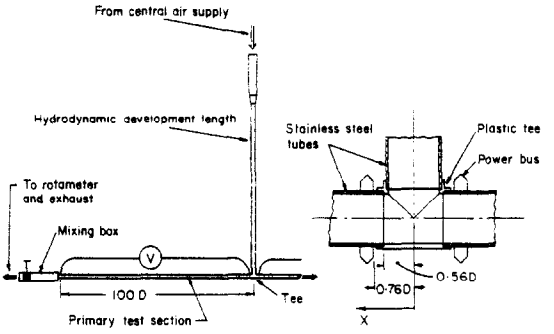

FIG. 1. Schematic diagrams of the experimental apparatus (left) and of the tee assembly (right).

The exhaust air was vented outside the laboratory. The orientation of the apparatus was as shown in the figure, that is, the hydrodynamic development tube was vertical and the heated test section tubes were horizontal.

The test sections and the development section were all cut from a single length of type 304 stainless steel tubing. The inner surface of each tube was honed to a very smooth satin finish. By use of a special gage, it was found that the flow cross section was perfectly circular to within 0.0005 cm (0.0002 in) over the entire length, with a mean diameter of 2.37 cm (0.933 in). The wall thickness was determined both by micrometer and optical comparator measurements, utilizing several pieces of the tubing. A small, but regular circumferential thickness variation was observed, and this is taken into account in the data reduction procedure. The mean wall thickness was 0.0894 cm (0.0352 in). Each of the heated test section tubes was 100 diameters in length whereas the hydrodynamic starting length was 90 diameters long. The tubes were hand straightened by a technique used for straightening firearm barrels.

The tee assembly is pictured schematically at the right of Fig. 1. The tee itself was fabricated by modifying one that was commercially available. With a view to avoiding spurious heat conduction which would give rise to uncertainties in the thermal boundary conditions, a thin-walled, non-metallic tee made of chlorinated polyvinyl chloride (cpvc) was employed. The I.D. of the tee was finished bored to the internal diameter of the stainless steel tubes. In addition, the axial length

of the tee was shortened to enable the heated test section tubes to be placed as close as possible to the center port. This was done to avoid possible ambiguities associated with redevelopment of the velocity field prior to the onset of heating. The test section and entrance length tubes were mated to the tee by means of lap joints, as illustrated in the figure.

Heating of the test sections was accomplished by passing electric current through the tube walls. In designing the bus bars and current carrying leads, consideration was given to avoiding extraneous heat conduction, both with respect to heat losses and to the circumferential temperature distribution in the tube wall. If a copper or aluminum ring had been affixed to the tube to convey the electric current, such a ring would have obliterated the circumferential temperature variations that might otherwise exist in the adjacent section of the tube owing to the fluid flow phenomena. In light of this, segmented copper rings were employed in lieu of continuous rings. Such a segmented ring was affixed to each end of the two heated tubes. Each ring had 12 segments.

Each segment mated with a 0.32-cm (1/8 in) copper rod whose function was to carry current to (or from) the segment. Each rod was fitted with a guard heater and a differential thermocouple. By adjustment of the guard heaters with the aid of the thermocouples, extraneous heat losses through the rods could be suppressed.

The relatively low resistance of the test section tubes ($\sim 0.024\,\Omega$) required a relatively high current (up to 100 A) to attain the power inputs corresponding to the desired bulk temperature rise ($\sim 14°C$ or 25°F). The current–voltage requirements were fulfilled by a power supply which consisted of a stabilized voltage source, an adjustable autotransformer, and a step-down power transformer.

The test section tubes and the hydrodynamic development length were each surrounded by a 30-cm (12 in) square plywood box whose function was to contain insulation. The insulated zone also encompassed the respective mixing boxes. Three different types of insulation were employed: silica aerogel, fiberglass, and blown cellulose. Although silica aerogel is the best insulator among these (thermal conductivity less than air), its exclusive use would have been prohibitively expensive. The aerogel, being a powder, was poured into the space adjacent to the tubes where the presence of thermocouples and other lead wires would have precluded the use of fibrous insulations.

As an additional precaution to minimize heat losses, the test section supports were fabricated from bakelite with knife-edge contacts.

Instrumentation

In expectation of both circumferential and axial variations of the heat-transfer coefficient, the test section tubes were heavily instrumented with thermocouples. A total of 142 thermocouples were affixed to each tube. At each of 17 axial stations between $X/D = 2$ and 60, eight thermocouples were deployed around the circumference with a uniform spacing of 45°. The first thermocouple station, $X/D = 2$, was situated 1.24 diameters downstream of the onset of heating (see Fig. 1). The successive thermocouple stations up to $X/D = 12$ were displaced from each other by a distance of two diameters, with larger spacings thereafter. Beyond $X/D = 60$, where circumferential uniformity was expected, only a single thermocouple was installed at each axial station. The thermocouple junctions were affixed to the tube surface with copper oxide cement, which is a good conductor of heat and a poor conductor of electricity. This latter attribute affords isolation between the direct current of the thermocouples and the alternating current passing through the test section tube.

The inlet bulk temperature of the air was measured by a four-prong thermocouple rake situated just upstream of the inlet cross section of the hydrodynamic development length. Similar rakes were employed to measure the bulk temperature at the exit of each of the heated test sections. To ensure the accuracy of the exit bulk temperature measurement, the thermocouple rake was placed just downstream of a mixing box made of pvc pipe fitted with three copper baffles.

All thermocouples were made from a calibrated roll of 36-gage iron–constantan wire. The thermocouple e.m.f.'s were read with the aid of a digital voltmeter to within one microvolt.

The flow rates through the test sections were measured with the aid of rotameters positioned downstream of the respective mixing boxes. Each rotameter had a rated capacity of 36 scfm. The rotameters were especially calibrated for the present experiments, thereby enabling them to be used with confidence in the low range of the scale as well as in the high range.

For the measurement of power input to the test sections, a 50:1 current transformer enabled the current to be measured by a laboratory grade ammeter with a 0–2 A range. The voltage drop across the test section, which never exceeded about 2.5 V, was read with the aid of a four-figure digital multimeter.

DATA REDUCTION

The evaluation of local heat-transfer coefficients from the measured outside tube wall temperatures and power inputs will now be described. Two types of heat-transfer coefficients will be considered. The first is the circumferentially local coefficient, that is, the coefficient which is specific to an angular position θ as well as to an axial station X. This quantity will be denoted by $h_x(\theta)$. The other is the circumferential average coefficient at an axial station X and is designated as $\bar{h}_x$. At sufficiently large downstream distances, where $\bar{h}_x$ becomes independent of X, it will be referred to as h_{fd} (fully developed).

The circumferentially local coefficient $h_x(\theta)$ is defined as

$$h_x(\theta) = \frac{q_x(\theta)}{T_{wx}(\theta) - T_{bx}} \tag{1}$$

where $q_x(\theta)$ and $T_{wx}(\theta)$ are, respectively, the local heat flux and local inside wall temperature at an angular

position θ, and T_{bx} is the bulk temperature. All of the aforementioned quantities are specific to an axial station X. The difference between the inside and outside wall temperatures depends on the level of the input power, but was typically a few hundredths of a degree Fahrenheit, which is at the threshold of the resolving power of the instrumentation. For completeness, the temperature difference across the wall was taken into account, although it had no influence on the results. The local bulk temperature was evaluated by adding the temperature rise due to heat addition to the inlet bulk.

To determine the local heat flux $q_x(\theta)$, an energy balance is made on an element of the tube wall. Such a balance includes the internal heat generation (ohmic heating), conduction in the tube wall, and heat losses through the insulation to the environment. The net axial conduction in the tube wall at locations in the thermal entrance region was estimated to be on the order of a few tenths of a percent of the internal heat generation and, on this basis, was neglected. (The net axial conduction in the fully developed region is zero.) Furthermore, owing to their small magnitude, radial temperature variations need not be considered in the energy balance for $q_x(\theta)$.

Consideration may then be given to an element which spans the thickness of the wall and subtends an angle $d\theta$. The axial length of the element is dX. Let R_i and R_o respectively denote the inner and outer radii, R_m the mean radius $=\frac{1}{2}(R_o+R_i)$, and t the wall thickness $=(R_o-R_i)$. An energy balance for such an element which takes account of the simplifications outlined in the foregoing paragraph is

$$[q_x(\theta)]R_i\,d\theta\,dX = q'''tR_m\,d\theta\,dX + k_w\frac{d}{d\theta}\left[\frac{t}{R_m}\frac{dT_{wx}}{d\theta}\right]d\theta\,dX - dQ_l \quad (2)$$

k_w is the thermal conductivity of type 304 stainless steel [7].

The volumetric heat generation rate q''' is assumed to be uniform throughout the tube wall and equal to the measured input power divided by the volume of the wall. The quantity dQ_l represents the heat loss to the environment. It can be written as

$$dQ_l = [T_{wx}(\theta) - T_\infty]\,d\theta\,dX/(\text{res}) \quad (3)$$

where T_∞ is the temperature of the environment, and (res) is the sum of the series thermal resistances of the insulation and the external natural convection. Upon substitution of equation (3) into (2) and after dividing through by $R_i\,d\theta\,dX$, an equation for evaluating $q_x(\theta)$ is obtained. Most of the inputs for the evaluation of $q_x(\theta)$ are straightforward, but the circumferential temperature derivatives and the wall thickness warrant some explanation.

To facilitate the determination of the temperature derivatives, the measured circumferential temperature distributions were fit with a trigonometric polynomial in the angular coordinate θ, with $\theta = 0$ at the 12 o'clock position on the tube circumference. In view of the near symmetry of the temperature distribution with respect to $\theta = 0$, a series involving even powers of the cosine was employed, that is

$$T_{wx}(\theta) = \tfrac{1}{2}a_0 + a_1\cos\theta + a_2\cos 2\theta \quad (4)$$

where the coefficients a_n are evaluated from [8]

$$a_n = (1/4)\sum_{j=1}^{8} T_{wx}(\theta_j)\cos n\theta_j \quad (5)$$

with $\theta_j = (j-1)\pi/4$. The $T_{wx}(\theta_j)$ appearing in equation (5) represent the measured temperature values.

With respect to the wall thickness, it was found by measurement that although both the inner and outer surfaces of the tube were nearly perfect circles (to within 0.0002 in), the centers of the respective circles were slightly displaced. This gave rise to a circumferential variation of the wall thickness that can be represented as

$$t = 0.0352 - 0.0022\cos\theta \quad (6)$$

where the values are in inches.

With equations (3)–(6) as input, the local heat flux was evaluated from (2). Then, in turn, the circumferentially local heat-transfer coefficient was computed from equation (1).

The circumferential average heat-transfer coefficient is defined here as

$$\bar{h}_x = \frac{\bar{q}_x}{\bar{T}_{wx} - T_{bx}} \quad (7)$$

in which

$$\bar{q}_x = (1/2\pi)\int_0^{2\pi} q_x(\theta)\,d\theta \quad (8)$$

$$\bar{T}_{wx} = (1/2\pi)\int_0^{2\pi} T_{wx}(\theta)\,d\theta = (1/8)\sum_{j=1}^{8} T_{wx}(\theta). \quad (9)$$

A dimensionless representation for $\bar{h}_x$ was achieved via the circumferential average Nusselt number $\overline{Nu}_x$

$$\overline{Nu}_x = \bar{h}_x D/k \quad (10)$$

where $D = 2R_i$, and k is the thermal conductivity of air at the local bulk temperature T_{bx}.

Two flow parameters will be employed in the presentation of the results. One of these is the Reynolds number Re_1 for the primary test section

$$Re_1 = 4\dot{m}_1/\mu\pi D. \quad (11)$$

The quantity $\dot{m}_1$ is the rate of mass flow in the primary test section, and μ is the viscosity of air evaluated at the mean of the inlet and outlet bulk temperatures. The second flow parameter is the flow split number S, which is defined as

$$S = \dot{m}_2/\dot{m}_1 \quad (12)$$

where the subscript 2 corresponds to the secondary test section. As indicated by equation (12), S represents the ratio of the mass flow in the secondary test section to that in the primary test section.

RESULTS AND DISCUSSION

The presentation of results will be subdivided into two sections. The first section is devoted to circumferential average Nusselt numbers and to related quantities such as thermal entrance lengths and fully

developed Nusselt numbers. The second section contains results for the circumferential variation of the heat-transfer coefficient.

Circumferential average Nusselt numbers; entrance lengths

The approach taken in presenting the circumferential average Nusselt number results is to focus on a specific primary Reynolds number Re_1 and to parametrically vary the flow split number S from zero to the maximum value consistent with the flow metering capacity in the secondary test section. For each Reynolds number and flow split number, $\overline{Nu}_x/Nu_{fd}$ is plotted as a function of the dimensionless axial coordinate X/D, where $X = 0$ is measured from the geometric center of the tee. The onset of heating is at $X/D = 0.76$. The use of $\overline{Nu}_x/Nu_{fd}$ as the presentation variable causes all of the curves to approach unity at sufficiently large X/D.

The results are presented in Figs. 2 and 3. The first of these is for primary Reynolds numbers of 47 900, 38 000 and 28 000. whereas the second gives results for

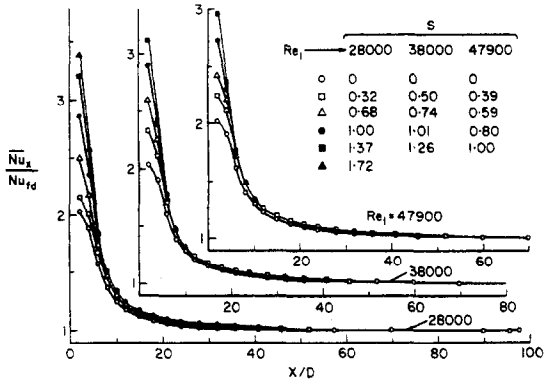

FIG. 2. Circumferential average Nusselt numbers, $Re_1 = 47\,900$, 38 000 and 28 000.

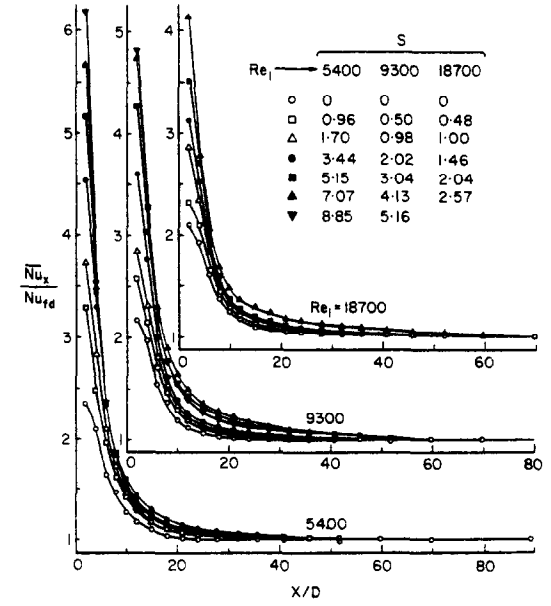

FIG. 3. Circumferential average Nusselt numbers, $Re_1 = 18\,700$, 9300 and 5400.

Reynolds numbers of 18 700, 9300 and 5400. Each of these figures is a composite of three graphs, with each graph corresponding to a specific Reynolds number. The various curves for each Reynolds number are parameterized by the flow split number S.

It is seen from the graphs that the axial distribution of $\overline{Nu}_x/Nu_{fd}$ has the same general character as that for the thermal entrance region of axisymmetric tube flows. That is, the Nusselt number has its largest value in the neighborhood of the inlet and decreases monotonically with increasing downstream distance, finally attaining a constant, fully developed value. Aside from this similarity in trend, there are important differences between the present results and those for conventional thermal entrance regions.

One major difference is in the magnitude of the $\overline{Nu}_x/Nu_{fd}$ ratio in the entrance region. To underscore this point, representative literature results for turbulent axisymmetric air flow in uniformly heated tubes are presented in Table 1. The Nusselt number ratios listed therein* correspond to an axial station that is 1.24 diameters downstream of the onset of heating. These results may be compared with those at the first measurement station of the present experiments. That station,

Table 1. Nu and $(X/D)_e$ information for axisymmetric air flow

Ref.	Type	Nominal Re	$(\overline{Nu}_x/Nu_{fd})_{1.24}$	$(X/D)_e$
[1]	Expt	$20–50 \times 10^3$	1.37	8–9
[9]	Expt	20×10^3	1.34	8
[10]	Expt	50×10^3	1.34	8
[11]	Anal	30×10^3	1.23	5
[12]	Anal	50×10^3	1.36	12

situated at $X/D = 2$ with respect to the geometric center of the tee, is also 1.24 diameters downstream of the initiation of heating.

Aside from that of [11], the $\overline{Nu}_x/Nu_{fd}$ of the table are about 1.35. These results are for an initially fully developed velocity profile. For simultaneously developing velocity and temperature fields, [1] and [11] give Nusselt number ratios of 1.50 and 1.37, respectively.

The aforementioned values may be contrasted with those of Figs. 2 and 3 at $X/D = 2$. It may be noted that at this station, the smallest Nusselt number ratios (those for $S = 0$) are in the range 2 to 2.35 whereas the largest ratio (at $S = 8.85$) is about 6.2. Clearly, the presence of the tee gives rise to substantially higher entrance region Nusselt numbers than are encountered in conventional pipe flows. Thus, the tee plays the role of an augmentation device.

There are a number of factors which contribute to the augmentation of the heat-transfer coefficients. One of these is the increased turbulence associated with the jet-like impingement and deflection that was mentioned in the Introduction. Another contributing factor

*The overbar on Nu_x is superfluous for the axisymmetric case, but is retained to be consistent with the notation used throughout the paper.

is the nature of the velocity distribution. In conventional axisymmetric pipe flows, the region of higher velocities is well away from the heat-transfer surface, i.e. from the wall. On the other hand, downstream of a tee with the inflow/outflow arrangement of the present experiments, there are regions of high velocity near the tube wall which, in effect, give rise to a scouring of the wall. Furthermore, with increasing S, the velocities which scour the wall are increased even though the primary Reynolds number Re_1 may be fixed. This is because the velocity of the fluid entering the tee is proportional to the sum of the mass flows $\dot{m}_1$ and $\dot{m}_2$ in the primary and secondary test sections. Thus, the entering velocity increases with S at a fixed value of Re_1, and this causes an increase in the velocity in the deflected flow.

The foregoing discussion points up the significant influence of the flow split parameter S on the entrance region Nusselt numbers. The range of S values that were attainable with the present instrumentation was different depending on the primary test section Reynolds number Re_1. At the lowest Re_1 value of the experiments ($Re_1 = 5400$), the range of S extended from zero to 8.85, whereas at the highest value of Re_1 ($Re_1 = 47\,900$), the range of S was from zero to one.

Examination of Figs. 2 and 3 indicates that in the initial portion of the entrance region, the Nusselt number distributions are arranged in a regular order as a function of S. In the intermediate and downstream portions of the entrance region, a number of trends are in evidence depending on the range of S. At the two largest Reynolds numbers, 47 900 and 38 000, where the range of S is essentially from zero to one, all of the curves for $S > 0$ merge into a single curve for $X/D > 8$. For $Re_1 = 28\,000$, where S ranges from zero to 1.72, there is a somewhat greater spread, although merging of curves is still in evidence. At $Re_1 = 18\,700$, the curves for the various S numbers are generally distinct from each other. Of particular interest is the relatively large spread between the curves for $S = 2.04$ and 2.57. Inasmuch as a similar spread occurs in this same range of S at other Reynolds numbers (e.g. between $S = 2.02$ and 3.04 for $Re_1 = 9300$), we believe that it is indicative of a change of flow regime. A second transition is also in evidence for the large S values which were attained at $Re_1 = 9300$ and 5400. For S greater than about 5, the curves actually dip below those for certain smaller S values.*

The nature of the aforementioned changes of flow regime cannot be identified with complete certainty. They may be related to laminar–turbulent transition in the wall jet that is formed downstream of the tee. Another possible factor is the collision of the two branches of the wall jet that respectively flow clockwise and counter-clockwise adjacent to the two vertical halves of the tube wall.

As a final item with respect to the $\overline{Nu}_x/Nu_{fd}$ ratios, it is interesting to compare the present results for the $S = 0$ case (no flow in the secondary test section) with those for a 90-degree mitered elbow. Measurements of the heat-transfer coefficients downstream of such an elbow were carried out in [2] and [3], respectively for water and air flows. Both investigations reported a maximum value of $\overline{Nu}_x/Nu_{fd}$ of about two. This compares very favorably with that for $S = 0$ in Figs. 2 and 3.

Attention will now be turned to another aspect of the distribution curves of Figs. 2 and 3, namely, the length of the thermal entrance region. The dimensionless thermal entrance length, $(X/D)_e$, will be defined here as the downstream distance from the geometric center of the tee where $\overline{Nu}_x/Nu_{fd} = 1.05$. The thermal entrance length results are plotted in Fig. 4 as a function of the flow split number S, with Reynolds number as a parameter. The data points have been interconnected by lines to provide continuity.

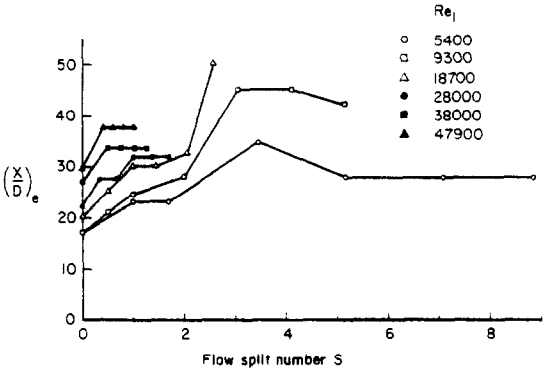

FIG. 4. Thermal entrance lengths.

To provide a baseline for comparison purposes, representative thermal entrance lengths for axisymmetric tube flows with an initially fully developed velocity profile are listed in Table 1. The consensus of the table is an $(X/D)_e$ of about eight. In contrast, the thermal entrance lengths of Fig. 4 are appreciably larger.* For the case of $S = 0$, where the smallest $(X/D)_e$ values of the present investigation are attained, the entrance lengths are 2 to $3\frac{1}{2}$ times larger than that of the axisymmetric tube flow. Even greater differences are in evidence for $S > 0$. These findings are consistent with the fact that substantial lengths are required to redevelop the complex flow field downstream of a tee.

Figure 4 indicates that the entrance lengths are larger at higher Reynolds numbers and vary in a rather complex manner with S. With increasing S, an initial increase in the entrance length is followed by another increase at the aforementioned first flow transition threshold and then by a decrease at the second flow transition threshold. Aside from these major features, there are minor local variations which are, in all likelihood, due to uncertainties in reading results from the relatively flat portions of the curves of Figs. 2 and 3.

*Specifically, the curves associated with S numbers greater than the second transition threshold dip below those for S values that exceed the first transition threshold.

*This conclusion is in no way affected by the slightly different definitions of $(X/D)_e$ in the figure ($X = 0$ at the center of the tee) and the table ($X = 0$ at the onset of heating).

Owing to this flatness, small uncertainties in $\overline{Nu}_x/Nu_{fd}$ are magnified in their effect on $(X/D)_e$.

As a final item with respect to the $\overline{Nu}_x$ results, brief mention may be made of the fully developed values, Nu_{fd}. At a fixed Reynolds number, the Nu_{fd} values for the various flow split runs never differed by more than 1% from their mean. Furthermore, the data agree to within 3% with the analytical predictions of (12) in the range above $Re_1 = 10000$ where the turbulence model of the analysis should be valid. It may also be noted that the energy balances were generally satisfied to within 1.5%.

Circumferential variations of the heat-transfer coefficient

There are two hydrodynamic phenomena which principally contribute to the circumferential variations of the heat-transfer coefficient. One is the wall jets created by the impingement–deflection process in the tee. The other is the recirculation zone situated in the upper part of the cross section at stations just downstream of the tee. The two phenomena are interrelated. The recirculation zone exists because the flow entering the tee impinges on the wall opposite the inlet port and is, therefore, concentrated adjacent to that wall (i.e. in the lower part of the cross section). The wall jets are fed by the deflection that takes place on the impingement wall. The wall jet that streams into the test section tube can be envisioned as being made up of two branches that respectively flow clockwise and counter-clockwise adjacent to the two vertical halves of the tube. This circumferential motion delivers substantial amounts of air from the lower part of the cross section, where it was initially concentrated, to the upper part of the cross section.

Although the causes of the circumferential variations can be identified, the details of their action (and interaction) are too complex to be explained without fluid flow measurements of the type reported in [5]. Of particular complexity is the response of the wall jet trajectory and of the position of the recirculation zone to changes in the flow split number S.

With this as background, the circumferential distributions of the heat-transfer coefficient $h_x(\theta)$ will now be presented. The results are given in terms of the ratio $h_x(\theta)/\bar{h}_x$, where $\bar{h}_x$ is the circumferential average coefficient at the axial station in question. The $h_x(\theta)/\bar{h}_x$ ratio will be plotted against the angular coordinate θ, where $\theta = 0$ is at the top of the tube and $\theta = \pi$ is at the bottom. Owing to symmetry, it will be sufficient to focus the discussion on the range between $\theta = 0$ and $\theta = \pi$.

The results for Reynolds numbers of 47900, 18700, 9300 and 5400 are presented in Figs. 5–8. Similar figures for $Re_1 = 38000$ and 28000, omitted here owing to space limitations, are available in [6] and show trends that essentially are identical to those for 47900. Each figure is subdivided into several graphs, each of which is for a fixed value of S. Results are given for axial stations $X/D = 2$, 4, 6, 8 and 60 in each graph.

The circumferential variations are seen to be confined to small values of X/D. In almost all cases, circumferential uniformity within $\pm 2\%$ of the mean is attained at $X/D = 8$. The most significant variations are those at the first measurement station, $X/D = 2$, where deviations as large as 30% from the mean are in evidence.

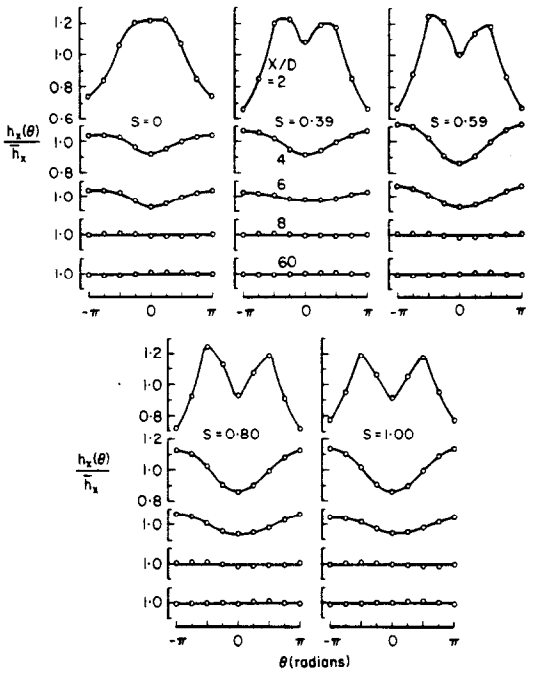

FIG. 5. Distributions of the local heat-transfer coefficient around the circumference of the tube, $Re_1 = 47900$.

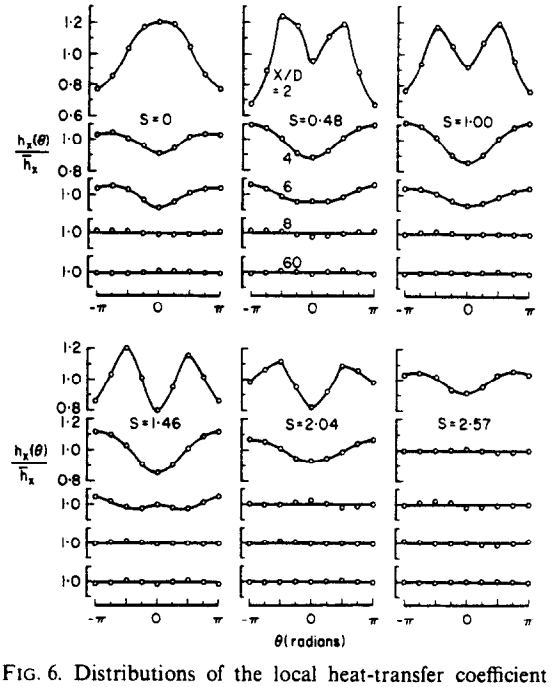

FIG. 6. Distributions of the local heat-transfer coefficient around the circumference of the tube, $Re_1 = 18700$.

The circumferential distribution curves at $X/D = 2$ are strongly influenced by the value of S. For $S = 0$, the maximum heat-transfer coefficient occurs at $\theta = 0$ (top of tube) and the minimum at $\theta = \pi$ (bottom of tube). Evidently, the circumferential transfer of air from

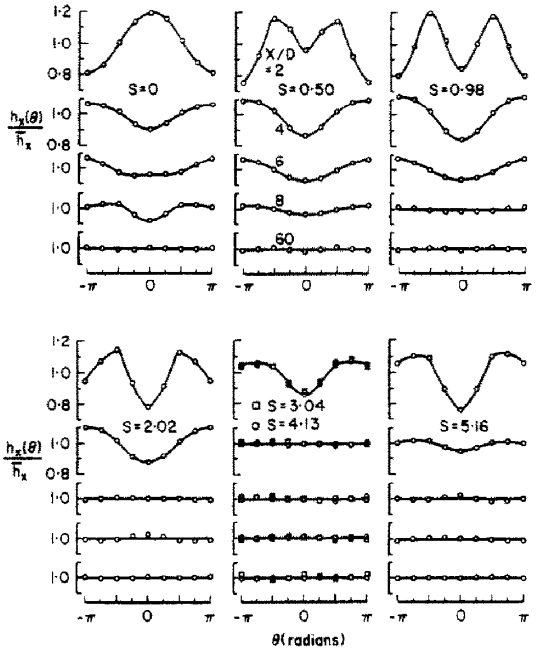

FIG. 7. Distributions of the local heat-transfer coefficient around the circumference of the tube, $Re_1 = 9300$.

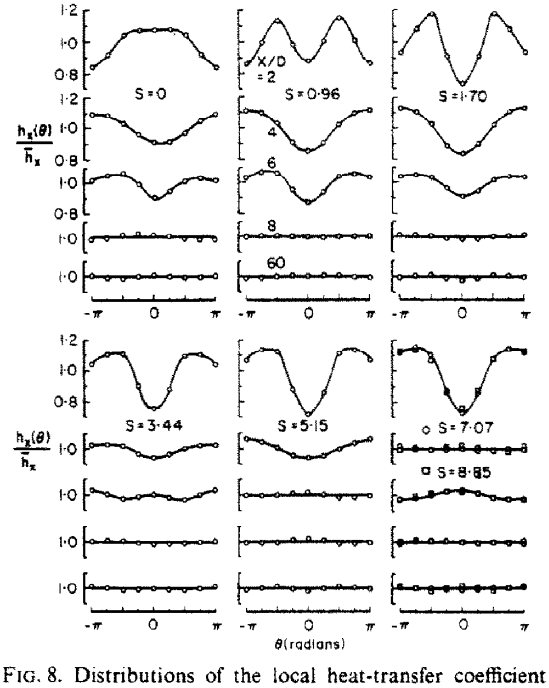

FIG. 8. Distributions of the local heat-transfer coefficient around the circumference of the tube, $Re_1 = 5400$.

the bottom of the tube to the top of the tube is highly efficient in this case. With increasing S, the maximum shifts toward the side of the tube, producing an "M"-shaped curve with minima at the top and bottom. When S surpasses a value of about two, a flattening occurs and the maximum moves nearer to the bottom of the tube (Figs. 6 and 7). Then, when S exceeds five, the minimum at $\theta = 0$ appears to deepen (Figs. 7 and 8). It is interesting to note that the S values of two and five correspond, more or less, to the two flow transition thresholds identified earlier. The variety of shapes evidenced by the distribution curves at $X/D = 2$ testifies to the complexity of the flow field.

The distribution curves at $X/D = 4$ and 6 are simpler in form and less responsive to variations of S. Typically, at these stations, the transfer coefficient attains its maximum value at the bottom of the tube and its minimum value at the top of the tube.

It was mentioned earlier that the circumferential distributions were insensitive to the Reynolds number in a certain range. This characteristic will now be examined in greater detail with the aid of Fig. 9. The figure

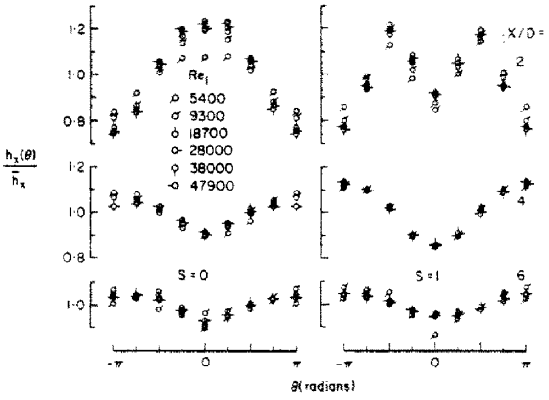

FIG. 9. Circumferential distributions of the heat-transfer coefficient for $S = 0$ and $S = 1$.

is subdivided into two halves, with the left half corresponding to $S = 0$ and the right half to $S = 1$. At $X/D = 2$, 4 and 6, $h_x(\theta)/\bar{h}_x$ distribution curves are plotted as a function of θ with the Reynolds number as a parameter. The data for Reynolds numbers between 18 700 and 47 900 are nearly coincident, with the maximum deviation of any data point from the mean in this range being less than 2%. The deviations increase at the lower Reynolds numbers, 9300 and 5400, although the trends are preserved. These deviations can be attributed to laminar flow effects. Figures similar to Fig. 9 are available in [6] for other values of S.

CONCLUDING REMARKS

It has been found that the presence of a flow-splitting tee at the inlet of a heated circular tube has a marked influence on the turbulent heat-transfer characteristics of the tube flow. These effects were investigated by systematically varying the flow split number S at each of six primary test section Reynolds numbers ranging from 5400 to 47 900.

The heat-transfer coefficients in the thermal entrance region were very much higher than those for conventional axisymmetric turbulent tube flows. At an axial station where $\overline{Nu}_x/Nu_{fd} \sim 1.35$ for a conventional flow, values of $\overline{Nu}_x/Nu_{fd}$ between two and six were attained in the presence of the tee, depending on the flow split number S. Thus, the tee plays the role of an augmentation device. Furthermore, the length of the thermal entrance region was substantially greater in the presence of a tee. Entrance lengths ranging from 17

to 50 diameters were encountered for the operating range of the present experiments, in contrast to the eight-diameter entrance length that is typical for axisymmetric flows.

Circumferential variations of the Nusselt number were found to be confined to the initial part of the entrance region, with circumferential uniformity being attained at a downstream length of about eight diameters. At the first measurement station (two diameters from the geometric center of the tee), the circumferential distributions exhibited deviations of up to 30% from the circumferential average. For a given flow split number, the circumferential distributions of $h_x(\theta)/\bar{h}_x$ were virtually independent of primary Reynolds numbers in the range from 18 700 to 47 900.

Both the circumferential average and circumferentially local heat-transfer results are suggestive of highly complex fluid flow phenomena.

REFERENCES

1. A. F. Mills, Experimental investigation of turbulent heat transfer in the entrance region of a circular conduit, *J. Mech. Engng Sci.* **4**, 63 (1962).
2. A. J. Ede and E. J. LeFevre, The effect of a right-angled bend on heat transfer in a pipe, in *International Developments in Heat Transfer*, Part III, p. 634. Amer. Soc. Mech. Engrs, New York (1961).
3. S. R. Tailby and P. W. Staddon, The influence of 90° and 180° pipe bends on heat transfer from an internally flowing gas stream, in *Proceedings of the Fourth International Heat Transfer Conference, Paris–Versailles*, Vol. 2, paper No. FC 4.5. A.S.M.E., New York (1970).
4. E. Achenbach, Mass transfer from bends of circular cross section to air, in *International Seminar on Future Energy Production—Heat and Mass Transfer Problems*, Dubrovnik, Yugoslavia (August 1975).
5. D. K. Kreid, C. J. Chung and C. T. Crowe, Measurements of the flow of water in a "T" junction by the LDV technique, *J. Appl. Mech.* **42**, 498 (1975).
6. D. A. Wesley, Heat transfer in a pipe downstream of a tee, Ph.D. Thesis, University of Minnesota (1976).
7. A. W. Black, The effect of circumferentially varying boundary conditions on turbulent heat transfer in a tube, Ph.D. Thesis, University of Minnesota (1966).
8. F. Scheid, *Theory and Problems of Numerical Analysis, Shaum's Outline Series*, p. 293. McGraw-Hill, New York (1968).
9. M. Hishida, Turbulent heat transfer and temperature distribution in the thermal entrance region of a circular pipe, *Bull. J.S.M.E.* **10**, 113 (1967).
10. H. Wolf, Heating and cooling air and carbon dioxide in the thermal entrance region of a circular duct, *J. Heat Transfer* **81C**, 267 (1959).
11. R. G. Deissler, Analysis of turbulent heat transfer and flow in the entrance regions of smooth passages, NACA TN 3016 (1953).
12. E. M. Sparrow, T. M. Hallman and R. Siegel, Turbulent heat transfer in the thermal entrance region of a pipe with uniform wall heat flux, *Appl. Scient. Res.* **A7**, 37 (1957). [See also *J. Heat Transfer* **82**, 152 (1960) and *Chem. Engng Sci.* **19**, 961 (1964).]

COEFFICIENTS LOCAUX ET GLOBAUX DE TRANSFERT TURBULENT DE CHALEUR SUR LA CIRCONFERENCE D'UNE TUBE EN AVAL D'UN TE

Résumé—Des expériences ont été effectuées afin de déterminer les coefficients de transfert de chaleur sur la circonférence et dans la longueur d'un tube chauffé situé en aval d'un té départageant l'écoulement. Dans la configuration utilisée l'air était délivré à la branche centrale du té après un long parcours d'établissement dynamique sans chauffage et ressortait du té par ses deux branches latérales. Des tubes chauffés identiques, comportant chacun un contrôle de débit, ont été adaptés à chaque section de sortie. L'un d'entre eux a été utilisé comme section test primaire. Les expériences ont été réalisées pour plusieurs nombres de Reynolds fixés dans la section test primaire, et à chaque nombre de Reynolds, l'écoulement à travers la sortie secondaire variait systématiquement. Les coefficients de transfert de chaleur, moyens sur la circonférence, dans la région d'établissement du régime thermique ont été trouvés nettement supérieurs à ceux obtenus en tube circulaire conventionnel. De plus, la longueur de la région d'établissement du régime thermique était très supérieure du fait de la présence du té. Les variations circonférencielles du coefficient de transfert de chaleur, sont limitées à la partie initiale de la région d'établissement, et une distribution circonférencielle uniforme était atteinte après huit diamètres au plus, comptés à partir du centre du té. Au niveau de la première section de mesure (située à deux diamètres du centre du té), les distributions circonférencielles présentaient des écarts atteignant 30 pour cent de la moyenne circonférencielle.

DIE LOKALEN UND MITTLEREN WERTE DES TURBULENTEN WÄRMEÜBERGANGSKOEFFIZIENTEN AM UMFANG EINES ROHRES HINTER EINER *T*-VERZWEIGUNG

Zusammenfassung—Es wurden Versuche zur Bestimmung des Wärmeübergangskoeffizienten am Umfang und längs eines beheizten Rohres, welches sich stromabwärts von einer *T*-Verzweigung befindet, durchgeführt. Die über eine unbeheizte hydrodynamische Anlaufstrecke dem *T*-Stück zugeführte Luft wurde über beide Enden des *T*-Stückes abgezogen. An die Ausgänge des *T*-Stückes wurden identische Heizrohre angeschlossen, welche beide mit einer Durchflußregelung versehen wurden. Eines der Heizrohre diente als Primär-Versuchsstrecke. Die Versuche wurden bei verschiedenen Reynoldszahlen in der Primärversuchsstrecke durchgeführt; bei jeder Reynoldszahl wurde die Strömung durch das Sekundär-Rohr systematisch variiert. Die über den Umfang gemittelten Wärmeübergangskoeffizienten in der thermischen Einlaufstrecke erwiesen sich als viel größer als bei konventionellen axialsymmetrischen Rohrströmungen. Durch das Vorschalten des *T*-Stückes wurde außerdem die thermische Einlauflänge wesentlich vergrößert. Eine Abhängigkeit der lokalen Wärmeübergangskoeffizienten vom Umfangswinkel war lediglich im ersten Teil der Einlaufstrecke zu beobachten; nach einem Abstand vom Mittelpunkt des *T*-Stückes, der etwa dem 8-fachen Rohrdurchmesser entsprach, konnten keine Unterschiede in den lokalen Wärmeübergangskoeffizienten mehr festgestellt werden. An der ersten Meßstelle (Entfernung zweifacher Durchmesser vom Mittelpunkt des *T*-Stückes) wichen die lokalen Wärmeübergangskoeffizienten bis zu 30% vom gemittelten Wert ab.

ЛОКАЛЬНЫЕ И СРЕДНИЕ КОЭФФИЦИЕНТЫ ТУРБУЛЕНТНОГО ТЕПЛОПЕРЕНОСА, ВНИЗ ПО ПОТОКУ ОТ *T*-ОБРАЗНОГО ВЫСТУПА В ТРУБЕ

Аннотация — Проводились эксперименты для определения коэффициентов теплопереноса как по окружности, так и вдоль участка нагреваемой трубы, расположенного вниз по потоку от *T*-образного выступа, разделяющего поток. Исследовался поток, в котором воздух подавался в центральную часть *T*-образного выступа по длинному ненагреваемому участку, где происходило гидродинамическое развитие течения, и выдувался через два концевых отверстия выступа. К каждому выходному отверстию были подведены одинаково нагреваемые трубки, имеющие свой регулятор расхода. Одна из нагреваемых трубок представляла собой основной экспериментальный участок. Опыты проводились при некоторых постоянных числах Рейнольдса для основного экспериментального участка. При всех числах Рейнольдса происходило систематическое измерение расхода через второе отверстие. Найдено, что средние коэффициенты теплопереноса по окружности в начальном участке нагрева существенно больше значений коэффициентов теплопереноса для обычного осесимметричного потока. Кроме того, длина начального обозреваемого участка существенно больше из-за наличия *T*-образного выступа. Изменения по окружности коэффициентов теплопереноса наблюдались только на начальном участке, а на расстоянии около 8 диаметров от центра *T*-образного выступа наблюдались равномерные распределения по окружности коэффициентов теплопереноса. На первой стадии измерений (два диаметра от центра *T*-образного выступа) отклонения распределений коэффициентов по окружности составляли 30% от средних значений.